Direct optical access to the triplet manifold of states in H_2

Ch. Jungen
Laboratoire Aimé Cotton du CNRS, Université de Paris-Sud, F-91405 Orsay, France
and Department of Physics and Astronomy, University College London, London WC1E 6BT, United Kingdom

M. Glass-Maujean
Laboratoire d'Etudes du Rayonnement et de la Matière en Astrophysique et Atmosphères,
Sorbonne Universités, UPMC Université Paris 06, CNRS, UMR 8112, F-75005 Paris, France
(Received 17 December 2015; published 22 March 2016)

A number of unassigned lines in the absorption spectrum of diatomic hydrogen are attributed to nominally forbidden transitions from the ground state to the nf manifold of states (Rydberg electron with $\ell = 3$ orbital momentum). They appear via weak $\ell-$ mixing interactions leading to local level perturbations. Our analysis is based on multichannel quantum defect theory and uses known theoretical information from the literature. The upper levels of most of these transitions are known to give rise to molecular fluorescence, and they are shown to be singlet-triplet mixed. We conclude that the well-known metastable $c\,^3\Pi_u^-$ state can be populated via one-photon absorption of uv photons followed by cascade emission $4f \rightarrow 3d \rightarrow 2p$.

DOI: 10.1103/PhysRevA.93.032514

H_2, the smallest stable molecule and the most abundant in the universe, is probably the molecular system that has been studied the most by spectroscopic methods. Its photoabsorption spectrum lies entirely in the vacuum-ultraviolet spectral region and has been the subject of a vast literature [1]. The accepted fact is that this spectrum corresponds to a united-atom type $s \rightarrow p$ excitation, which is split in the molecule into a very large number of rovibronic components and blurred by strong "nonadiabatic" rovibronic interactions. These latter couple the electronic and nuclear degrees of freedom and dominate the unimolecular decay once the excitation energy exceeds the dissociation and ionization thresholds, via predissociation and autoionization processes.

Among the thousands of known absorption transitions that have been successfully interpreted within this conceptual framework, about a dozen have resisted analysis—some of them for over forty years [2], whereas a number of them has been discovered recently [3]. In this paper we assign the majority of these "extra lines" by showing that they arise via combined partial wave (ℓ orbital angular momentum) mixing and hyperfine-induced singlet-triplet mixing. These transitions provide a direct photoallowed route into the triplet manifold of H_2. This finding opens up interesting possibilities for laser-induced production of metastable triplet H_2, and it might also have implications in astrophysics.

Specifically we demonstrate here that the extra lines of the H_2 photoabsorption spectrum are $nf \leftarrow X\,^1\Sigma_g^+$ transitions (where f refers to the $\ell = 3$ orbital angular momentum of the photoexcited electron), which appear through the weak nonspherical $p \sim f$ interaction. Moreover we show below that because the *ortho* f levels—levels corresponding to two parallel proton spins—are strongly singlet-triplet mixed, they provide a route to the triplet manifold of states of H_2. In particular, it must be possible to populate metastable triplet states by absorption of a single photon by the singlet ground state, via cascade photoemission transitions in the excited states.

The absorption spectrum of H_2 is a many-line spectrum, with no recognizable band structure appearing, and has since the early times been assignable only with the help of theoretical calculations [2]. These have evolved toward ever increasing sophistication and have nowadays attained a predictive power which for moderate vibrational excitation and $n \leqslant 4$ in H_2 is better than ≈ 1 cm^{-1}, and which is even more accurate for higher n values (see [1,4] and references therein). Specifically, the calculations are carried out using multichannel quantum defect theory (MQDT)[5–7], which is a generalized version of scattering theory, extended to include bound states ("closed" channels) in addition to continua ("open" channels). In the present application we disregard all open channels and initially also spin effects, by considering the spectrum of excited H_2 as consisting of quasidiscrete singlet levels.

The power of MQDT derives from the fact that it is able to bridge the gap between the traditional Born-Oppenheimer approach—in which the nuclei are assumed to move more slowly than the electrons due to their larger mass—and the opposite regime of entirely nonadiabatic motion, where it is the excited Rydberg electron that is moving slowly compared to the rotating and vibrating nuclear frame owing to its large distance from the residual ion core $H_2{}^+$. MQDT bridges the gap between the two regimes by use of a so-called frame transformation [8,9]. In this scheme—and neglecting rotational motion for the simplicity of the argument—the vibrational-electronic reaction matrix elements are

$$K_{v^+v^{+\prime}} = \tan\left[\int \chi_{v^+}(R)\pi\mu_{\ell\ell'}^{(\lambda)}(R)\chi_{v^{+\prime}}(R)dR\right], \qquad (1)$$

where R is the internuclear distance, $\chi_{v^+}(R)$ and $\chi_{v^{+\prime}}(R)$ are ion core vibrational wave functions coupled by vibronic interaction, and $\tan\pi\mu_{\ell\ell'}^{(\lambda)}(R)$ is a purely electronic clamped-nuclei scattering matrix describing the electron scattering off the ion core with the nuclei kept fixed in space. λ is the molecular symmetry (component of the orbital angular momentum along the molecular axis). MQDT procedures match the short-range wave functions implied by the reaction matrix $\mathbf{K}$ of Eq. (1) for a given total energy E to asymptotically correctly behaving

electron Coulomb wave functions by requiring [6]

$$\det|\mathbf{K} + \tan\beta(E)| = 0\,. \tag{2}$$

$\beta(E)$ is an asymptotic phase vector whose components $\beta_{v^+}(E)$ for closed channels take values $\beta_{v^+}(E) = \pi\nu_{v^+}$ with $\nu_{v^+} = (2^{-\frac{1}{2}})[E_{v^+} - E]^{-\frac{1}{2}}$, the effective principal quantum number corresponding to that channel. If the quantization condition Eq. (2) is applied using the fixed-nuclei elements $\tan\pi\mu^{(\lambda)}_{\ell\ell'}(R)$, the clamped-nuclei potential energy curves of the given symmetry are recovered. If it is enforced using the vibronic matrix Eq. (1), the spectrum of vibronic levels is obtained including the vibronic dynamics involving the Rydberg channels corresponding to ℓ and ℓ'. This methodology has been described in numerous papers and several reviews [5–7].

Figure 1 is a synthetic spectrum calculated using the energy- and internuclear distance-dependent quantum defects corresponding to $\ell = 1$ $p\sigma$, $p\pi$ and $\ell = 3$ $f\sigma$, $f\pi$, $f\delta$, and $f\phi$ channels. The quantum defects $\mu^{(\lambda)}_{i,j}(E,R)$ have been taken from the literature [10]. Dipole transition moment functions $d_{\epsilon p\lambda\leftarrow X}(E,R)$ have been taken from quantum-chemical calculations [11] and converted to the form required for the MQDT following the method of Ref. [12]. The transition moments towards the $\ell = 3$ channels, $d_{\epsilon f\lambda\leftarrow X}$, have been set to zero because we know [11] that near the ground state equilibrium position $R \approx 1.4$ a.u., their ratio f/p is $\approx 10^{-2}$, resulting in absorption line intensities (Einstein A coefficients) that are $\approx 10^4$ times weaker for $f \leftarrow X$ than for $p \leftarrow X$ absorption transitions. The spectrum of Fig. 1(a) contains more than 5 000 transitions and the enlarged sections shown

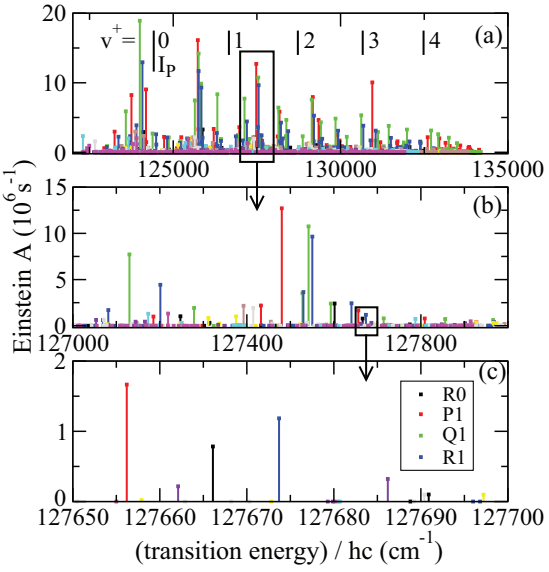

FIG. 1. (a) Theoretical MQDT absorption spectrum of H_2 from 1 22 000 to 11 35 000 cm^{-1} (15.1 to 16.7 eV). Rydberg levels np, v^+ with $n \leqslant 32$ and $v^+ \leqslant 10$ are included in the calculations. Rotational transitions $P(N'')$, $Q(N'')$, and $R(N'')$ with $N'' \leqslant 3$ are included assuming room temperature. The color coding is indicated in panel (c) for $N'' = 0$ and 1. The lowest vibrational ionization thresholds H_2^+, v^+ are indicated at the top. (b), (c) Enlarged sections as indicated by the boxes in (a) and (b), respectively.

in Figs. 1(b) and 1(c) underline its erratic appearance as a many-line spectrum showing no obvious Rydberg series. Transitions corresponding to different initial levels N'' in the $X\,^1\Sigma_g^+, v'' = 0$ ground state—assumed to be in equilibrium at room temperature—and to different excited-state rotational quantum numbers N are indicated in different colors.

Our hypothesis here is the following: We assume that absorption transitions involving $\ell = 3$ upper levels can arise only via *intensity borrowing*, when an upper $\ell = 3$ level nearly coincides with an $\ell = 1$ level having the same angular momentum N and total parity, and interacts with it via the weak $p \sim f$ coupling. This coupling has been determined in Ref. [10] by recording and analyzing millimeter-wave spectra involving p and f Rydberg states with $n \approx 60$. The analysis fully accounted for the hyperfine interactions in these highly excited states. The $p \sim f$ coupling is indeed very weak; it amounts to only $\approx 6 \times 10^{-4}$ on an absolute (quantum defect) scale near $R \approx 2$ a.u., which implies interaction matrix elements $H_{nf\sim n'p}$ of the order ≈ 2 cm^{-1} when $n \sim n' \sim 4$ as might typically be observed in Refs. [2] and [3]. Our multichannel quantum defect calculations therefore should be just accurate enough—at least for the lower half of the spectrum shown in Fig. 1(a)—to identify perturbation-induced weak $nf \leftarrow$ X transitions.

Specifically we proceed as follows: We carry out two full MQDT calculations covering the range shown in Fig. 1(a), one in which the $p \sim f$ interaction is set to zero and one in which it is included. The direct absorption strength $f \leftarrow X$ is set to zero in both calculations, so that the corresponding transitions can appear only via local perturbations. We next subtract the two synthetic spectra from each other, searching for the small differences that appear due to the $p \sim f$ coupling. As the overall intensity must be conserved, there will be negative as well as positive differences, whereby the latter correspond to nf levels which gained intensity by intensity borrowing from the former, which lose a corresponding amount on account of the interaction.

The result of this procedure is displayed in the difference spectrum of Fig. 2. The positions of the filled colored circles indicate the intensity gain or loss for every transition when the $p \sim f$ mixing is included in the MQDT calculation. The figure also displays the positions of the observed unidentified spectral lines from Table I as vertical bars. It may be seen at once that many—albeit not all—of the unidentified lines are in more or less close coincidence with predicted extra lines involving f upper levels that appear via the $p \sim f$ channel interaction. Panels (b) and (c) of Fig. 2 are zooms demonstrating how the unidentified transition at 123 708.6 cm^{-1} can be assigned as an $R(0)$ transition and how the observed transition at 126 362.6 cm^{-1} can be assigned as a $Q(1)$ transition. These transitions are seen to emerge in the calculations from the large number of spectral lines whose intensity is not perturbed by the weak $p \sim f$ interaction, and which therefore are placed near the abscissa in the difference plots of Fig. 2.

The final assignments are given in Table I, which also identifies the main channel component of each upper level. It may be seen that up to 130 000 cm^{-1} we have assigned all lines with the exception of the transition at 123 864.9 cm^{-1} which remains unidentified. The residuals observed-calculated are ≈ 1 cm^{-1} at the lower end of the spectrum, but, as expected,

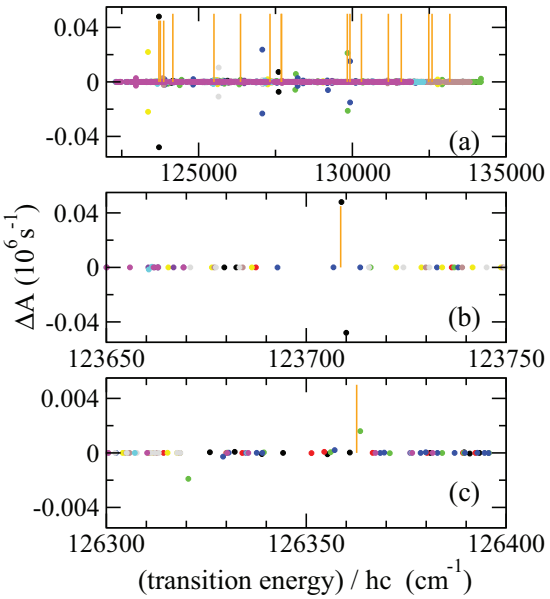

FIG. 2. Vertical lines (orange): Unidentified absorption lines from Table I. Filled circles: Difference of theoretical MQDT spectra obtained with and without mixing of p and f channels (color coding as in Fig. 1). Positive entries denote transitions to f levels that have gained intensity. Negative entries correspond to the loss of intensity of transitions to p levels. (a) Full range 1 22 000–1 35 000 cm^{-1} (15.1–16.7 eV) as in Fig. 1(a). (b), (c) Enlarged sections showing the identification of an $R(0)$ and a $Q(1)$ transition, respectively.

the agreement deteriorates as the energy increases. We have not been able to assign any of the transitions above 130 000 cm^{-1}. Levels belonging to the $4f$ manifold of states have been identified previously [13,14] in $5g$-$4f$ and $4f$-$3d$ infrared emission transitions, but were limited to levels with $v^+ \leqslant 2$, i.e., lower than the assignments made in Table I. Indirect support for our assignments comes from the fact that the "donor" transitions, that lend intensity to the extra lines, are indeed observed to be weakened by the $p \sim f$ interaction: Whereas overall the *ab initio* MQDT approach [12] accounts for observed line intensities quantitatively to within ±20% even when ℓ mixing is neglected, we find that the donor transitions of the ten assigned extra lines listed in Table I are indeed on the average observed 30% weaker than predicted by the same theory (cf. Table 3 of [15]). Our calculations indicate that most of the donor transitions are related to the "acceptor" transitions according to $n' = n$ and $v^{+'} = v^+$.

TABLE I. Extra lines in H_2 absorption. Transition energies ν/c in cm^{-1} from $v'' = 0, N''$. Crosses (x) designate transitions that have been observed to give rise to molecular fluorescence. $R(N''), Q(N''), P(N'')$ indicate the assignment to transitions with $N - N'' = +1$, 0, and -1. N^+ is the ion core rotational angular momentum.

Transition	Ref.			Obs-Calc	Upper state
1 23 708.6	[2]		R(0)	− 0.2	$5f, v^+ = 3, N^+ = 2$
1 23 754.1	[2]		P(1)	+2.0	$6f, v^+ = 1, N^+ = 3$
1 23 864.9	[2]				
1 24 162.0	[2]		R(0)	+0.7	$4f, v^+ = 3, N^+ = 4$
1 25 499.0	[3]	x	Q(3)	+0.1	$4f, v^+ = 4, N^+ = 5$
1 26 362.6	[3]	x	Q(1)	− 0.8	$5f, v^+ = 3, N^+ = 3$
1 27 320.6	[3]		Q(1)	− 3.3	$4f, v^+ = 5, N^+ = 3$
1 27 692.7	[3]		R(0)	+3.9	$6f, v^+ = 3, N^+ = 2$
1 28 160.9	[3]	x	Q(1)	− 0.9	$5f, v^+ = 4, N^+ = 3$
1 29 834.9	[3]	x	Q(1)	− 7.9	$5f, v^+ = 5, N^+ = 3$
1 29 921.7	[3]	x	R(1)	− 2.7	$6f, v^+ = 4, N^+ = 5$
1 30 294.9	[3]				
1 31 170.4	[3]	x			
1 31 590.9	[3]				
1 32 483.7	[3]				
1 32 591.5	[3]				
1 33 168.1	[3]				

Further evidence for the correctness of the present assignments comes from the fact that excitation of some of the extra lines listed in Ref. [3] has been observed to give rise to molecular fluorescence. This means that their upper levels are sufficiently long-lived (⩾1 ns) to emit a photon. As the full spectral range shown in Figs. 1 and 2 lies higher than the dissociation limit $H(1s) + H(n = 2)$ and most of it lies above the ionization potential ($I_p = 124\,417.5$ cm^{-1}, cf. Fig. 1), the upper levels of all extra lines except the lowest three are subject to autoionization as well as predissociation, processes that are generally fast and are known to quench fluorescence altogether. Exceptions—for superexcited levels in any molecule as far as we are aware—are the $Q(N'')$ transitions in H_2 which in many cases give rise to fluorescence, via their pure $^1\Pi_u^-$ symmetry upper levels, because the vibronic coupling affecting them is extremely weak [16]. Indeed, the quantum defect $\mu_{\ell\ell}^{(\Pi)}$ has almost no $R-$ dependence so that the off-diagonal elements of K in Eq. (1) are very small in such a way that the radiative decay route has a chance to compete. With this in mind we should expect that the extra lines giving rise to molecular fluorescence turn out to be Q transitions; it is satisfying to see (Table I) that with a single exception this is indeed the case.

The fluorescing upper nf levels excited by Q absorption transitions are ortho levels and possess a hyperfine structure which we have not considered so far in the present calculations, but which theoretically and experimentally is well understood from the study of millimeter-wave [10] inter-Rydberg optical transitions. There are two limiting coupling cases which may occur, referred to as Hund's coupling cases (b) and (e) [17,18], which prevail depending on whether the singlet-triplet splitting dominates, or whether the ion core spin (hyperfine) structure dominates, respectively. This is illustrated schematically in Fig. 3. Here on the left the familiar case (b) structure of the H_2 $2p\pi$ $C\ ^1\Pi_u^-$ and $c\ ^3\Pi_u^-$ is shown with the total electron spin S a well-defined quantum number. Spin-spin and hyperfine interactions split the $N = 1$ levels into J and F components, giving altogether 10 hyperfine components. While the singlet-triplet separation of the $2p\pi$ C and c states amounts to about 4 200 cm^{-1}, it is as small as 0.07 cm^{-1} in the $4f$ manifold of levels [10,14] and smaller in the $5f$ and $6f$ manifolds; in other words, it is comparable to the H_2^+ ion hyperfine splitting which is of the order of 0.04 cm^{-1}. As a result, the level structure departs towards the Hund's case (e) scheme depicted on the right-hand side of Fig. 3, where the total spin G^+ of the ion core, the sum of the electron and nuclear spins, is well defined, and it is the weak coupling of the spin of the nonpenetrating

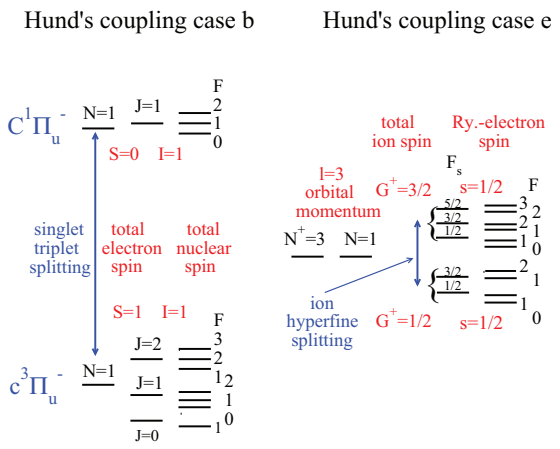

FIG. 3. Fine and hyperfine structure of $N = 1$ ortho levels of H_2 (+ total parity, antisymmetric) in Hund's coupling cases (b) (left) and (e) (right) (schematic). The angular momenta which are successively coupled to the spinless molecule are indicated in red, the resulting quantum number immediately to the right, in black. S, total electron spin; I, total nuclear spin; G^+, total ion spin (electron plus nuclei); F_s, total angular momentum without Rydberg electron spin; and s, Rydberg electron spin.

Rydberg $4f$ electron which causes the hyperfine structure to appear.

These considerations imply that the fluorescing ortho nf levels excited by the Q absorption transitions are *singlet-triplet mixed*. To ascertain this, we have carried out MQDT test calculations, based on the approach of Ref. [10], in which all spins were included. The results indeed confirm that there is significant singlet-triplet mixing in the $4f$ manifolds. The molecular fluorescence of these excited levels therefore must take place *in parallel* in the singlet as well as in the triplet manifolds. It follows further that by cascade photon emissions, e.g., $4f \rightarrow 3d \rightarrow 2p$, the metastable $c\,^3\Pi_u^-$ state may be populated.

The above conclusions could be checked experimentally by vacuum-ultraviolet (vuv) laser action spectroscopy, aided by the fact that the $4f$-$3d$ and $3d$-$2p$ triplet emission transitions of H_2 are well known through Fourier-transform spectroscopy [19,20]. In a broader context, it would seem interesting to explore whether the excitation pathway of triplet H_2 identified here could play a role in the photon-induced chemistry of the interstellar medium.

We thank Dr. S. T. Pratt (Argonne) for helpful comments on the manuscript. C.J. was supported in part by the Ernst Miescher Fonds, Freiwillige Akademische Gesellschaft Basel, Switzerland.

[1] M. Glass-Maujean *et al.*, J. Mol. Spectrosc. **293-294**, 19 (2013).
[2] G. Herzberg and C. Jungen, J. Mol. Spectrosc. **41**, 425 (1972).
[3] M. Glass-Maujean, C. Jungen, G. Reichardt, A. Balzer, H. Schmoranzer, A. Ehresmann, I. Haar, and P. Reiss, Phys. Rev. A **82**, 062511 (2010).
[4] J. Z. Mezei *et al.*, J. Chem. Phys. **141**, 064305 (2014).
[5] C. H. Greene and C. Jungen, Adv. At. Mol. Phys. **21**, 51 (1985).
[6] *Molecular Applications of Quantum Defect Theory*, edited by C. Jungen, Vol. 1 (The Institute of Physics, Bristol, 1996).
[7] C. Jungen, in *Handbook of High Resolution Spectroscopy*, edited by M. Quack and F. Merkt (Wiley, Chichester, 2011), Vol. 1, Chap. Elements of quantum defect theory, p. 471.
[8] U. Fano, Phys. Rev. A **2**, 353 (1970).
[9] C. Jungen and O. Atabek, J. Chem. Phys. **66**, 5584 (1977).
[10] A. Osterwalder *et al.*, J. Chem. Phys. **121**, 11810 (2004).
[11] L. Wolniewicz and G. Staszewska, J. Mol. Spectrosc. **220**, 45 (2003).
[12] M. Glass-Maujean and C. Jungen, J. Phys. Chem. A **113**, 13124 (2009).
[13] G. Herzberg and C. Jungen, J. Chem. Phys. **77**, 5876 (1982).
[14] D. Uy *et al.*, J. Chem. Phys. **113**, 10143 (2000).
[15] M. Glass-Maujean *et al.*, J. Mol. Spectrosc. **293-294**, 1 (2013).
[16] M. Glass-Maujean, C. Jungen, H. Schmoranzer, A. Knie, I. Haar, R. Hentges, W. Kielich, K. Jankala, and A. Ehresmann, Phys. Rev. Lett. **104**, 183002 (2010).
[17] G. Herzberg, in *Molecular Spectra and Molecular Structure* (van Nostrand Reinhold, New York, 1950), Vol. I.
[18] C. Jungen and G. Raseev, Phys. Rev. A **57**, 2407 (1998).
[19] C. Jungen *et al.*, J. Chem. Phys. **93**, 2289 (1990).
[20] D. Bailly and M. Vervloet, Mol. Phys. **105**, 1559 (2007).